Journal of Neuroscience Research 88:3566–3577 (2010)

The Wheat Germ Agglutinin-Fractionated Proteome of Subjects With Alzheimer's Disease and Mild Cognitive Impairment Hippocampus and Inferior Parietal Lobule: Implications for Disease Pathogenesis and Progression

Fabio Di Domenico,[1] Joshua B. Owen,[2] Rukhsana Sultana,[2] Rena A. Sowell,[2] Marzia Perluigi,[1] Chiara Cini,[1] Jian Cai,[3] William M. Pierce,[3] and D. Allan Butterfield[2]*

[1]Department of Biochemical Sciences, Sapienza University of Rome, Rome, Italy
[2]Department of Chemistry, Center of Membrane Sciences, and Sanders-Brown Center on Aging, University of Kentucky, Lexington, Kentucky
[3]Department of Pharmacology, University of Louisville, Louisville, Kentucky

Lectin affinity chromatography is a powerful separation technique that fractionates proteins by selectively binding to specific carbohydrate moieties characteristic of protein glycosylation type. Wheat germ agglutinin (WGA) selectively binds terminal N-acetylglucosamine (O-GlcNAc) and sialic acid moieties characteristic of O-linked glycosylation. The current study utilizes WGA affinity chromatography to fractionate proteins from hippocampus and inferior parietal lobule (IPL) from subjects with Alzheimer's disease (AD) and arguably its earliest form, mild cognitive impairment (MCI). Proteins identified by proteomics that were fractionated from MCI and AD hippocampus by WGA affinity chromatography with altered levels compared with age-matched controls included GP96, γ-enolase, glutamate dehydrogenase, glucosidase IIα, 14-3-3ε, 14-3-3γ, 14-3-3ζ, tropomyosin-2, calmodulin 2, gelsolin, β-synuclein, α1-antichymotrypsin, and dimethylguanosine tRNA methyltransferase. Proteins identified by proteomics that were fractionated from MCI and AD IPL by WGA affinity chromatography showing altered levels compared with age-matched controls included protein disulfide isomerase, calreticulin, and GP96. The proteins described in this study are involved in diverse processes, including glucose metabolism, endoplasmic reticulum (ER) functions, chaperoning, cytoskeletal assembly, and proteolysis, all of which are affected in AD. This study, the first to use proteomics to identify WGA-fractionated proteins isolated from brains from subjects with MCI and AD, provides additional information about the active proteome of the brain throughout AD progression.

Key words: proteomics; wheat germ agglutinin; lectin affinity chromatography; mass spectrometry; Alzheimer's disease; amnestic mild cognitive impairment

Alzheimer's disease (AD) is a neurodegenerative disorder that currently affects 5.3 million Americans and in the absence of interventions to slow or halt progression of this dementing disorder is predicted to affect 16–20 million Americans in just a few decades (Mebane-Sims, 2009). AD is the most common cause of dementia and is characterized pathologically by the occurrence of neurofibrillary tangles (NFTs) and senile plaques (SPs) in the neocortex, entorhinal cortex, and hippocampus (Markesbery, 1997). In addition, the aforementioned brain regions as well as hippocampal efferents to the inferior parietal lobule (IPL) are dramatically atrophied in AD brain compared with the brains from nondemented subjects (Clower et al., 2001). NFTs occur intracellularly and feature paired helical filament (PHF) structures composed of hyperphosphorylated tau, whereas senile plaques are extracellular and are composed primarily of amyloid-beta peptides (Aβs). Aβs contained in SPs range between 39 and 43 amino acids in length, the Aβ 1–42 variant being the dominant form present in the plaques (Selkoe, 2004). Amnestic mild cognitive impairment (aMCI) is arguably

Fabio Di Domenico and Joshua B. Owen contributed equally to this work.

Contract grant sponsor: NIH; Contract grant number: AG-05119 (to D.A.B.); Contract grant number: AG-10836 (to D.A.B.); Contract grant sponsor: Istituto Pasteur—Fondazione Cenci Bolognetti (to F.D.D.).

*Correspondence to: Prof. D. Allan Butterfield, Department of Chemistry, Center of Membrane Sciences, and Sanders-Brown Center on Aging, University of Kentucky, Lexington, KY 40506. E-mail: dabcns@uky.edu

Received 15 June 2010; Revised 28 August 2010; Accepted 3 September 2010

Published online 8 October 2010 in Wiley Online Library (wileyonlinelibrary.com). DOI: 10.1002/jnr.22528

the earliest form of AD. aMCI patients have detectable deficits in speech, memory, or other essential cognitive abilities but no dementia; however, these deficits do not interfere with activities of daily living (Mebane-Sims, 2009). Estimates suggest that 10–20% of the population aged 65 and older has aMCI, and a significant portion of aMCI patients progresses further to AD (Mebane-Sims, 2009). The clinical involvement of patients diagnosed with aMCI is a vital focus of AD research.

Protein glycosylation is a posttranslational modification (PTM) that affects proteins in a variety of ways, including proper protein folding, protein function regulation, and cellular localization. Protein glycosylation occurs in two general forms, N-linked glycosylation and O-linked glycosylation. N-linked glycosylation occurs in the endomembrane system and has a canonical serine/threonine (Ser/Thr)-X-asparagine (Asn) motif to which glycans are added to the Asn residue. O-linked glycosylation is the addition of carbohydrates to Ser or Thr residues; however, O-linked glycosylation sites do not have a well-characterized motif for glycan addition. O-linked glycosylation has traditionally been thought to occur only in the Golgi apparatus as part of the secretory pathway, but studies show that O-linked glycosylation occurs on cytoplasmic and nucleoplasmic proteins through the addition of a single N-acetylglucosamine (O-GlcNAc) residue to Ser/Thr (Hart, 1997; Hart et al., 2007). The exact role of nonsecretory pathway O-linked glycosylation is unknown, but studies suggest that nucleoplasmic and cytoplasmic O-linked glycosylation works in concert with phosphorylation to regulate proteins (Hart et al., 2007). Additionally, nonsecretory pathway O-link glycosylation has been hypothesized to function as a cellular glucose sensor (Lefebvre et al., 2010). Levels of nonsecretory pathway O-linked glycosylation are decreased globally in AD, including levels of O-GlcNAc modified tau protein (Liu et al., 2004).

Lectin affinity chromatography is a powerful separation technique that fractionates proteins by selectively binding to specific carbohydrate moieties characteristic of protein glycosylation type. Concanavalin-A (ConA) and wheat germ agglutinin (WGA) are the two most widely used lectins for chromatographic separations. ConA has affinity for high-mannose and terminal glucose carbohydrates that are commonly found in N-linked glycoproteins. In addition, ConA contains a binding site with an affinity for excessively hydrophobic proteins. WGA selectively binds terminal N-acetylglucosamine (O-GlcNAc) and sialic acid moieties characteristic of O-linked glycosylation. The addition of O-GlcNAc occurs in both secretory and nonsecretory O-linked glycosylation. Previous studies from our laboratory utilized ConA to fractionate proteins from MCI and AD hippocampus and inferior parietal lobule (IPL; Owen et al., 2009). The current study explores the glycoproteome of MCI and AD hippocampus and IPL using WGA lectin affinity chromatography coupled to two-dimensional (2D) gel proteomics techniques.

TABLE I. MCI and AD Subject Profiles

	Age (years)	Sex	Brain weight (g)	PMI (hr)	Braak stage
Control 1	93	Female	1,080	2.75	2
Control 2	74	Male	1,140	4.00	1
Control 3	86	Female	1,150	1.75	1
Control 4	76	Female	1,315	2.00	1
Control 5	79	Male	1,240	1.75	2
Control 6	86	Female	1,300	3.75	1
Average	82 ± 7.2		1,204 ± 95	2.67 ± 1.01	1.33 ± 0.52
MCI					
MCI 1	99	Female	930	2.00	5
MCI 2	88	Female	1,080	2.25	5
MCI 3	87	Male	1,200	3.50	4
MCI 4	87	Male	1,170	2.25	3
MCI 5	91	Female	1,155	5.00	3
MCI 6	82	Female	1,075	3.00	3
Average	89 ± 5.7		1,102 ± 98	3.0 ± 1.1	3.8 ± 1.0
Control 1	77	Male	1,310	3.50	1
Control 2	83	Male	1,275	2.00	3
Control 3	87	Male	1,150	2.00	2
Control 4	72	Male	1,150	3.75	1
Control 5	85	Female	1,020	2.50	3
Control 6	81	Male	1,410	2.00	2
Average	81 ± 5.5		1,219 ± 139	2.60 ± 0.8	2.00 ± 0.9
AD 1	80	Female	1,160	2.75	6
AD 2	90	Female	1,050	2.60	6
AD 3	88	Male	1,230	5.75	5
AD 4	81	Male	1,260	3.00	6
AD 5	81	Female	835	3.00	6
AD 6	92	Female	1,090	2.00	6
Average	85 ± 5.3		1,104 ± 154	3.2 ± 1.3	5.8 ± 0.4

MATERIALS AND METHODS

Sample Preparation

Hippocampus and IPL samples (n = 6 each) from well-characterized subjects with AD and MCI and age-matched controls (Table I) were obtained from the University of Kentucky Alzheimer's Disease Clinical Center Neuropathology Core. Samples were homogenized on ice with sucrose isolation buffer [0.32 M sucrose with protease inhibitors, 4 μg/ml leupeptin, 4 μg/ml pepstatin A, 0.125 M Tris, pH 8.0, 5 μg/ml aprotinin, 0.2 mM phenylmethylsulfonylfluoride (PMSF), and 0.6 mM $MgCl_2$]. Table I presents demographic data for the MCI and AD subjects. Note the very short post-mortem interval of these samples.

Protein estimation and WGA Lectin Affinity Columns

Protein concentrations were determined using the BCA method, and aliquots (1,500 μg) were diluted with 5× binding/wash buffer in a 4:1 volumetric ratio and loaded into WGA affinity columns. WGA lectin columns, binding/wash, and elution buffers were prepared as described in the manufacturer's instructions (Pierce Biotechnology, Rockford IL). The samples were loaded onto columns and incubated for 10 min with end-over-end mixing using an elliptical rotor. The samples were spun at 1,000*g* for 1 min, the effluent was reloaded onto the

columns, and the process was repeated. The effluent was discarded after this step. Binding/wash buffer (400 μl) was added to the WGA lectin columns, and the columns then were centrifuged at 1,000*g* for 1 min, and the process was repeated. The columns were loaded with elution buffer (200 μl) and incubated for 10 min with end-over-end mixing using an elliptical rotor. The samples were spun at 1,000*g* for 1 min, and the effluent was retained. This process was repeated, and the elution buffers containing the WGA-associated proteins were combined (400 μl) and concentrated (to ~ 25 μl) using 30-kDa cut-off filters (Millipore, Billerica MA). Protein concentration was redetermined using the BCA method, and the remaining aliquots were suspended in 200 μl of rehydration buffer composed of a 1:1 ratio (v/v) of the Zwittergent solubilization buffer (7 M urea, 2 M thiourea, 2% Chaps, 65 mM DTT, 1% Zwittergent 0.8% 3–10 ampholytes, and bromophenol blue) and ASB-14 solubilization buffer [7 M urea, 2 M thiourea 5 mM TCEP, 1% (w/v) ASB-14, 1% (v/v) Triton X-100, 0.5% Chaps, 0.5% 3–10 ampholytes] for 2 hr.

First-Dimension Electrophoresis

For the first-dimension electrophoresis, approximately 50 μg of protein in 200 μl of sample buffer was applied to 110-mm pH 3–10 ReadyStrip IPG strips (Bio-Rad, Hercules CA). The strips were then actively rehydrated in the protean isoelectric focusing (IEF) cell (Bio-Rad) at 50 V for 18 hr. The isoelectric focusing was performed at increasing voltages as follows; 300 V for 1 hr, then linear gradient to 8,000 V for 5 hr, and finally 20,000 V/hr. Strips were then stored at –80°C until the second-dimension electrophoresis was performed.

Second-Dimension Electrophoresis

For the second dimension, the IPG strips, pH 3–10, were thawed and equilibrated for 10 min in 50 mM Tris-HCl (pH 6.8) containing 6 M urea, 1% (w/v) sodium dodecyl sulfate (SDS), 30% (v/v) glycerol, and 0.5% dithiothreitol, and then reequilibrated for 15 min in the same buffer containing 4.5% iodacetamide instead of dithiothreitol. Linear gradient precast criterion Tris-HCl gels (8–16%; Bio-Rad) were used to perform second-dimension electrophoresis. Precision Protein Standards (Bio-Rad) were run along with the samples at 200 V for 65 min.

Sypro Ruby Staining

After the second-dimension electrophoresis, the gels were incubated in fixing solution (7% acetic acid, 10% methanol) for 20 min and stained overnight at room temperature with 50 ml Sypro ruby gel stain (Bio-Rad). The Sypro ruby gel stain was then removed, and gels were stored in deionized water.

WGA Affinity Experiments

WGA glycoprotein affinity was tested by the addition of ethylenediamine tetracetic acid (EDTA; 500 mM) to column washing and elution buffers provided in the WGA lectin kit (Pierce Biotechnology). MCI age-matched control hippocampus samples were homogenized on ice with sucrose isolation buffer [0.32 M sucrose with protease inhibitors, 4 μg/ml leupeptin, 4 μg/ml pepstatin A, 0.125 M Tris, pH 8.0, 5 μg/ml aprotinin, 0.2 mM phenylmethylsulfonylfluoride (PMSF), 0.6 mM $MgCl_2$, and 500 mM EDTA]. These samples underwent WGA column chromatography as described above. Protein fractions were loaded onto linear gradient 18-well precast criterion Tris-HCl gels (8–16%; Bio-Rad) and were used to perform one-dimensional electrophoresis. Precision Protein Standards (Bio-Rad) were run along with the sample at 120 V for 120 min. Gels were visualized using a STORM phosphoimager as described above.

Image Analysis

Sypro ruby-stained gel images were obtained using a STORM phosphoimager as indicated above and saved in TIFF format. Gel imaging was software-aided using PD-Quest (Bio-Rad) imaging software. Briefly, a master gel was selected, followed by normalization of all gels (control and AD or control and MCI) according to the total spot density. Gel to gel analysis was then initiated in two parts. First, manual matching of common spots that could be visualized among the differential 2D gels was performed. After obtaining a significant number of spots, the automated matching of all spots was then initiated. Automated matching is based on user-defined parameters for spot detection. These parameters are based on the faintest spot, the largest spot, and the largest spot cluster that occur in the master gel and are defined by the user. Based on these parameters, the software defines spot centers for the gel. If the software ''misses'' spots that are obvious to the naked eye, the user can manually assign a spot center. This process generates a large pool of data, approximately 350 spots. Only proteins showing computer-determined significant differential levels between the two groups being analyzed were considered for identification. To determine significant differential levels of proteins, analysis sets were created using the analysis set manger software incorporated into the PD-Quest software. The numbers of pixels that occur in a protein spot were computed by the software corresponding to an increase/decrease in protein level. A quantitative analysis set was created that recognized matched spots with differences in the numbers of pixels that occur in each spot, and a statistical analysis set was created that used a Student's *t*-test at 95% confidence to identify spots with P values of $P < 0.05$. Spots with $P < 0.05$ were considered significant. A Boolean analysis set was created that identified overlapping spots from the aforementioned quantitative and statistical sets. These spots were selected for subsequent mass spectrometric analysis.

In-Gel Trypsin Digestion

Protein spots statistically different from controls were digested in-gel by trypsin using protocols previously described and modified by Thongboonkerd et al. (2002). Spots were taken from individual gels and were not pooled for mass spectrometric analysis. The amount of protein from one gel-spot is sufficient for identification. Briefly, spots of interest were excised using a clean blade and placed in Eppendorf tubes, which were then washed with 0.1 M ammonium bicarbonate (NH_4HCO_3) at room temperature for 15 min. Acetonitrile was then added to the gel pieces and incubated at room temperature for 15 min. This solvent mixture was then removed, and gel

pieces were dried. The protein spots were then incubated with 20 μl of 20 mM DTT in 0.1 M NH_4HCO_3 at 56°C for 45 min. The DTT solution was removed and replaced with 20 μl of 55 mM iodoacetamide in 0.1 M NH_4HCO_3. The solution was then incubated at room temperature for 30 min. The iodoacetamide was removed and replaced with 0.2 ml of 50 mM NH_4HCO_3 and incubated at room temperature for 15 min. Acetonitrile (200 μl) was added. After 15 min of incubation, the solvent was removed, and the gel spots were dried in a flow hood for 30 min. The gel pieces were rehydrated with 20 ng/μl modified trypsin (Promega, Madison, WI) in 50 mM NH_4HCO_3 with the minimal volume enough to cover the gel pieces. The gel pieces were incubated overnight at 37°C in a shaking incubator.

All the mass spectrometry results reported in this study were obtained in collaboration with the Department of Pharmacology in the University of Louisville Mass Spectrometry Facility. Part of the results, MCI hippocampus and IPL, has been obtained using A Bruker Autoflex matrix-assisted laser desorption ionization-time of flight (MALDI-TOF) coupled with the MASCOT search engine. The data from AD hippocampus and IPL were acquired using a Nanomate Orbitrap XL MS platform that generate MS/MS spectra analyzed using the SEQUEST database. The use of two mass spectrometers and databases for protein identification was due to the MALDI-TOF instrument being replaced by the Orbitrap instrument during the course of the project.

Mass Spectrometry 1

A Bruker Autoflex MALDI-TOF mass spectrometer in the reflectron mode was used to generate peptide mass fingerprints (Bruker Daltonic, Billerica, MA). Peptides resulting from in-gel digestion with trypsin were analyzed on a 384-position, 600-μm AnchorChip Target (Bruker Daltonics, Bremen, Germany) and prepared according to AnchorChip recommendations (AnchorChip Technology, Rev. 2, Bruker Daltonics, Bremen, Germany). Briefly, 1 μl of digestate was mixed with 1 μl of alpha-cyano-4-hydroxycinnamic acid (0.3 mg/ml in ethanol: acetone, 2:1 ratio) directly on the target and allowed to dry at room temperature. The sample spot was washed with 1 μl of a 1% TFA solution for approximately 60 sec. The TFA droplet was gently blown off the sample spot with compressed air. The resulting diffuse sample spot was recrystallized (refocused) using 1 μl of a solution of ethanol: acetone:0.1% TFA (6:3:1 ratio). Reported spectra are a summation of 100 laser shots. External calibration of the mass axis was used for acquisition and internal calibration using either trypsin autolysis ions or matrix clusters and was applied post-acquisition for accurate mass determination. Peptide mass fingerprinting was used to identify proteins from tryptic peptide fragments by utilizing the MASCOT search engine based on the entire NCBI and SwissProt protein databases. Database searches were conducted allowing for up to one missed trypsin cleavage and using the assumption that the peptides were monoisotopic, oxidized at methionine residues, and carbamidomethylated at cysteine residues. Mass tolerance of 150 ppm, 0.1-Da peptide tolerance, and 0.2-Da fragmentation tolerance were the window of error allowed for matching the peptide mass values. Probability-based MOWSE scores were estimated by comparison of search results against estimated random match population and were reported as $-10 \cdot \log10\ (p)$, where p is the probability that the identification of the protein is a random event. MOWSE scores greater than 63 were considered to be significant ($P < 0.05$). All protein identifications were in the expected size and isoelectric point (pI) range based on the position in the gel.

Mass Spectrometry 2

Protein spots of interest were excised and subjected to in-gel trypsin digestion, and resulting tryptic peptides were analyzed with an automated nanospray Nanomate Orbitrap XL MS platform. The Orbitrap MS was operated in a data-dependent mode whereby the eight most intense parent ions measured in the FT at 60,000 resolution were selected for ion trap fragmentation with the following conditions: injection time 50 msec, 35% collision energy. MS/MS spectra were measured in the FT at 7500 resolution, and dynamic exclusion was set for 120 sec. Each sample was acquired for a total of ~ 2.5 min. MS/MS spectra were searched against the ipi_Human Database using SEQUEST with the following criteria: Xcorr > 1.5, 2.0, 2.5, 3.0 for +1, +2, +3, and +4 charge states, respectively, and P value (protein and peptide) < 0.01. IPI accession numbers were cross-correlated with SwissProt accession numbers for final protein identification.

Immunoprecipitation

For immunoprecipitation experiments, 150 μg protein extracts was suspended in 500 μl RIPA buffer (10 mM Tris, pH 7.6; 140 mM NaCl; 0.5% NP40 including protease inhibitors) and then incubated with 1 μg monoclonal antibody against 14-3-3γ protein (wild-type-specific PAb11; Santa Cruz Biotechnology, Santa Cruz, CA) at 4°C overnight. Immunocomplexes were collected using protein A/G suspension for 2 hr at 4°C and washed five times with immunoprecipitation buffer. Immunoprecipitated 14-3-3γ was recovered by resuspending the pellets in loading buffer, and protein was detected by Western blot.

Western Blot

Aliquots of the immunoprecipitated samples containing 50 μg of protein were added to sample buffer, denaturated for 5 min at 100°C, loaded on 8–16% precast Criterion gels (Bio-Rad) and separated by electrophoresis at 100 mA for 2 hr. The gels were then transferred to nitrocellulose paper using the Transblot-BlotSD Semi-DryTransfer Cell at 20 mA for 2 hr. Subsequently, the membranes were blocked at 4°C for 1 hr with fresh blocking buffer made of 3% bovine serum albumin (BSA) in phosphate-buffered saline containing 0.01% (w/v) sodium azide and 0.2% (v/v) Tween 20 (PBST). The membranes were incubated with anti-14-3-3γ (Santa Cruz Biotechnology) primary antibody (1:1,000) for expression analysis and anti-β-O-linked N-acetylglucosamine (Sigma-Aldrich, St. Louis, MO) primary antibody (1:1,000) for glycosylation analysis in PBST for 2 hr with gentle rocking at room temperature. The membranes were then washed three times for 5 min each with PBST, followed by incubation

with anti-mouse alkaline phosphatase or horseradish peroxidase-conjugated secondary antibody (1:3,000) in PBST for 2 hr at room temperature. Membranes were then washed three times in PBST for 5 min and developed using or 5-bromo-4-chloro-3-indolyl-phosphate/nitroblue tetrazolium (BCIP/NBT) color developing reagent for alkaline phosphatase secondary antibody or ECL plus WB detection reagents for horseradish peroxidase-conjugated secondary antibody. Blots were dried and scanned in TIF format using Adobe Photoshop on a Canoscan 8800F (Canon) or STORM UV transilluminator (λex = 470 nm, λem = 618 nm; Molecular Dynamics, Sunnyvale, CA) for chemiluminescence. The images were quantified with ImageQuant TL 1D version 7.0 software (GE Healtcare).

Statistical Analysis

Statistical analysis of protein levels matched with spots on 2D gels from AD and MCI hippocampus and inferior parietal lobule compared with age-matched controls were carried out using Student's *t*-tests. A value of $P < 0.05$ was considered statistically significant (see above under Image analysis for generation of analysis sets). Only proteins that were considered significantly different by Student's *t*-test were subjected to in-gel trypsin digestion and subsequent proteomic analysis. According to Maurer and Peters (2005), generalized statistical tests that apply to proteomics studies are unavailable. Becauise of the small numbers of proteins that are typically identified in proteomics studies compared with microarray data, statistical methods applied to thousands of hits in microarray studies are not applicable for proteomics studies with relatively small numbers of identified proteins. Hence, Student's *t*-test was used for analysis (Boguski and McIntosh, 2003; Maurer and Peters, 2005).

RESULTS

Column Specificity Experiment

The specificity of the WGA column for carbohydrate moieties was tested using EDTA to poison the column's lectin domain. The addition of EDTA to the equilibration and wash buffers used in the chromatography experiment successfully blocked protein binding of the lectin domain (Fig. 1), indicating that nonspecific binding to the WGA column did not occur.

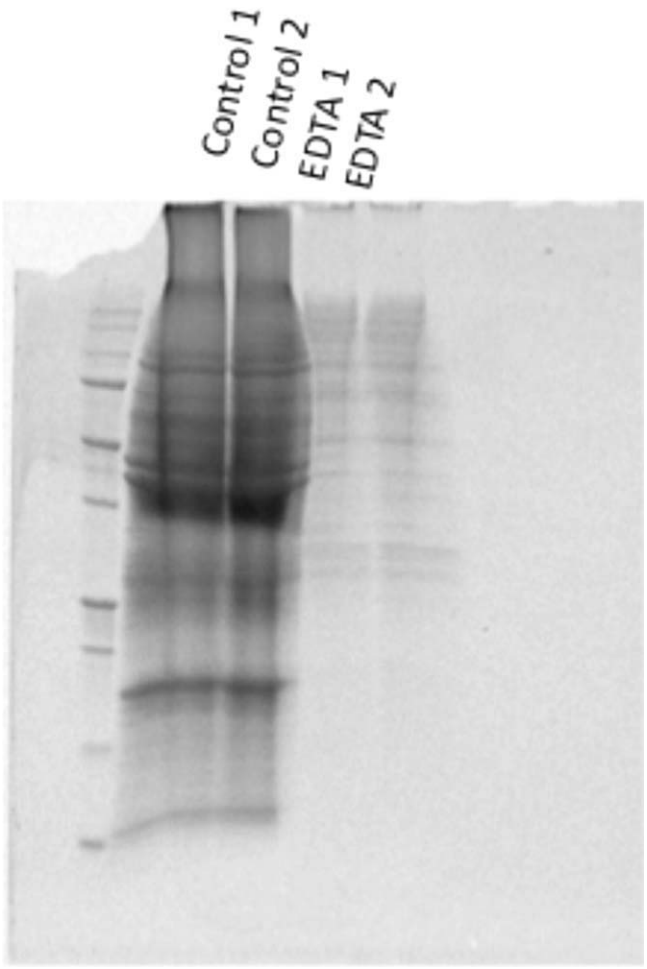

Fig. 1. EDTA-based column specificity 1D gel image. Lanes 1 and 2 are control samples treated with all buffers as described in Materials and Methods. Lanes 3 and 4 represent control samples in which all buffers described in Materials and Methods include 500 mM EDTA. EDTA acts as an inhibitor of lectin binding domains, and the resulting loss of signal shows that the WGA column binds proteins through the lectin binding domain with no nonspecific binding.

MCI vs CTR Hippocampus and IPL

Seven proteins with altered WGA affinity were identified in aMCI hippocampus, and one protein was altered in aMCI IPL compared with age-matched controls. -Fold change values are expressed as disorder (aMCI or AD) relative to age-matched control (CTR; e.g., 0.66-fold decrease of GP96 in MCI hippocampus signifies that the levels of GP96 WGA affinity is 0.66 times lower in MCI hippocampus than age-matched control. 14-3-3ε Showed a 2.43-fold increase in WGA affinity and signifies that the level of 14-3-3ε WGA affinity is 2.43 times higher in MCI hippocampus than age-matched control; see Table II). Compared with control, decreased WGA affinity in hippocampus was shown for GP96 (0.66-fold), glucosidase IIα (0.48-fold), and γ-enolase (0.16-fold), whereas WGA affinity was significantly increased for 14-3-3ε (2.43-fold), 14-3-3γ (1.66-fold), glutamate dehydrogenase (11.5-fold), and tropomyosin 2 (2.30-fold; Table II, Fig. 2). Protein disulfide isomerase showed increased WGA affinity in aMCI IPL (2.16-fold) compared with age-matched controls (see Table II, Fig. 2).

AD vs. CTR Hippocampus and IPL

Nine proteins with altered WGA affinity were identified in AD hippocampus and two in AD IPL. 14-3-3ζ (2.07-Fold), tropomyosin 1 (2.08-fold), glutamate dehydrogenase (2.66-fold), α1-antichymotrypsin (5.50-fold), and *N*2,*N*2-dimethylguanosine tRNA methyltransferase (DMGtRNAMT; 1.70-fold) showed an increase in WGA affinity in AD hippocampus. In contrast, calmodulin

TABLE II. Summary of Mass Spectrometry-Based Characterization of WGA-Fractionated Proteins in MCI and AD

NCBI GI No.	NCBI Accession No.	Protein/accession	Coverage (%)	pI, Mr (Da)	Mowse score[1]/ probability score[2]	Fold increase/ decrease in WGA affinity[3]	*P* value[4]	Disorder/brain region
15010550	AAK74072.1	GP96	24	4.73, 90,309	177[1]	0.66 Decrease	0.05	MCI/HP
2274968	CAA04006.1	Glucosidase IIα	13	5.74, 107,263	115[1]	0.48 Decrease	0.05	MCI/HP
5803011	NP_001966.1	γ-Enolase	51	4.91, 47,450	231[1]	0.16 Decrease	0.01	MCI/HP
5803225	NP_006752.1	14-3-3ε	60	4.76, 26,658	178[1]	2.43 Increase	0.02	MCI/HP
48428721	P61981.2	14-3-3γ	41	4.80, 28,235	112[1]	1.66 Increase	0.01	MCI/HP
4885281	NP_005262.1	Glutamate dehydrogenase	25	7.66, 61,701	103[1]	11.5 Increase	0.02	MCI/HP
6573280	AAF17621.1	Tropomyosin 2	32	4.70, 29,980	124[1]	2.30 Increase	0.01	MCI/HP
20070125	NP_000909.2	Protein disulfide isomerase	17	4.76, 57,480	71[1]	2.16 Increase	0.03	MCI/IPL
21735625	NP_663723.1	14-3-3ζ	21	4.57, 27,728	1.00e–005[2]	2.07 Increase	0.04	AD/HP
136083	P13104.1	Tropomyosin 1	4	4.55, 32,723	5.00e–007[2]	2.08 Increase	0.04	AD/HP
4502549	NP_001734.1	Calmodulin	28	3.93, 16,827	3.00e–009[2]	0.5 Decrease	0.03	AD/HP
4885281	NP_005262.1	Glutamate dehydrogenase	14	7.66, 61,360	3.00e–009[2]	2.66 Increase	0.03	AD/HP
5803011	NP_001966.1	γ-Enolase	64	4.76, 47,240	3.00e–015[2]	0.14 Decrease	0.03	AD/HP
50659080	NP_001076.2	α1-Antichymotrypsin	20	5.22, 47,621	3.00e–007[2]	5.50 Increase	0.04	AD/HP
121116	P06396.1	Gelsolin	10	5.86, 85,645	1.00e–0002[2]	0.44 Decrease	0.01	AD/HP
12230777	Q9V1P3.1	Dimethylguanosine tRNA methyltransferase	4	8.59, 43,192	1.00e–009[2]	1.7 Increase	0.02	AD/HP
2501105	Q16143.1	β-Synuclein	10	4.26, 14,280	1.00e–0007[2]	0.13 Decrease	0.02	AD/HP
15010550	AAK74072.1	GP96	19	4.73, 90,309	118[1]	2.00 Increase	0.04	AD/IPL
62897681	BAD96780.1	Calreticulin	21	4.30, 47,061	86[1]	16.0 Increase	0.02	AD/IPL

[1]Proteins of interest were identified using MASCOT database searches following MALDI-TOF mass spectrometry. Mowse scores are associated with protein identification using the MASCOT database search algorithm. Scores >63 are considered significant.

[2]Proteins of interest were identified using SEQUEST database searches following Orbitrap MS/MS mass spectrometry. The probability scores associated with protein identification using the SEQUEST search algorithm.

[3]Fold changes are expressed as disorder (aMCI or AD) relative to age-matched control. (i.e., 0.66-fold decrease of GP96 in MCI hippocampus is equivalent to 44% of the degree of GP96 WGA affinity in MCI hippocampus than age-matched control. 14-3-3ε Showed a 2.43-fold increase in WGA affinity and signifies that the degree of 14-3-3ε WGA affinity is 2.43 times higher in MCI hippocampus than age-matched control).

[4]The *P* value associated with the -fold changes observed between disorder and brain region with respect to appropriate nondemented age-matched controls using Student's *t*-test.

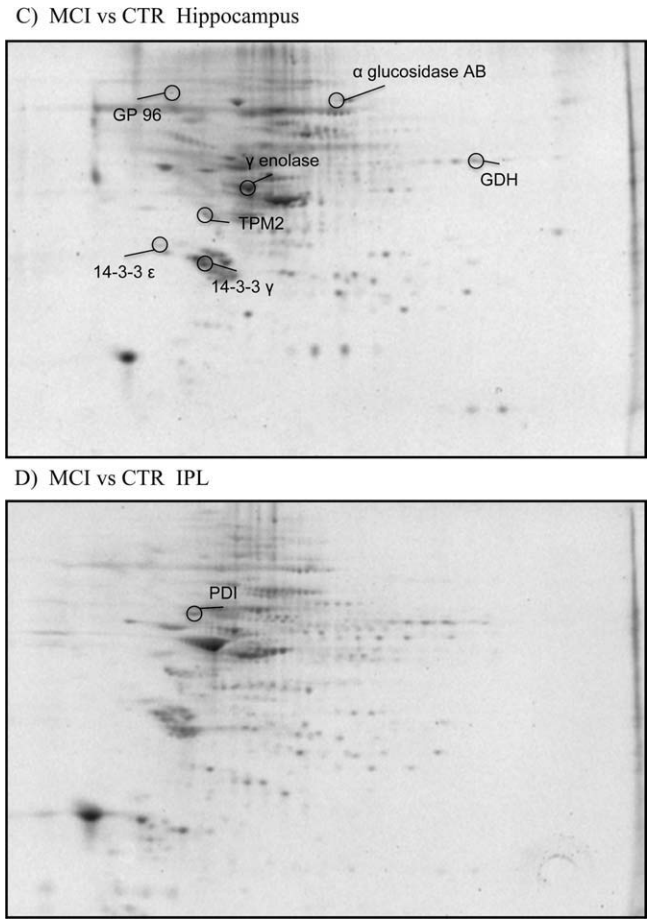

Fig. 2. Sypro-stained 4–16% polyacrylamide representative 2D gels of WGA-eluted proteins from MCI hippocampus and IPL and age-matched control with statistically significant protein spot identities. For protein spot *P* values refer to Table II.

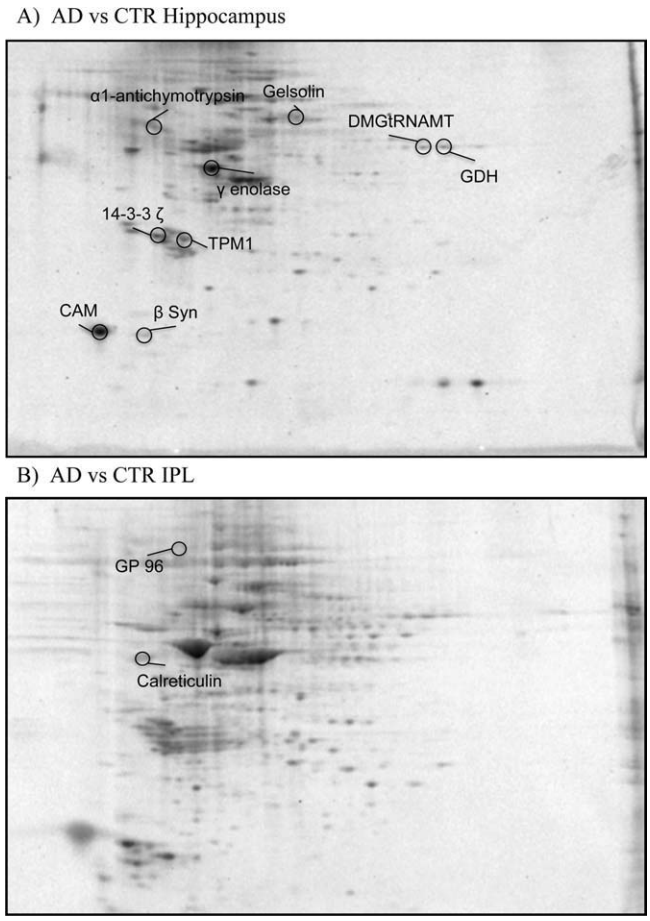

Fig. 3. Sypro-stained 4–16% polyacrylamide representative 2D gels of WGA-eluted proteins from AD hippocampus and IPL and age-matched control with statistically significant protein spot identities. For protein spot *P* values refer to Table II.

(0.50-fold), γ-enolase (0.14-fold), gelsolin (0.44-fold), and β-synuclein (0.13-fold) were found with decreased WGA affinity in AD compared with CTR samples (Table II, Fig. 3). Both calreticulin (16.0-fold) and GP 96 (2.00-fold) showed an increase in WGA affinity in AD IPL in comparison with age-matched CTR samples (Table II, Fig. 3).

Confirmation of O-GlcNAc Glycosylation on 14-3-3γ

To ascertain the implications of increased WGA affinity, a validation study on 14-3-3γ glycosylation using traditional immunochemistry was performed. Western blot analysis showed that overall levels of 14-3-3γ were not significantly different between CTR and MCI hippocampus (Fig. 4A). However, increased levels of N-acetylglucosamine linked to the proteins in MCI sample vs. CTR, in agreement with the proteomic results, was observed (Fig. 4B). Both techniques demonstrate that 14-3-3γ is differentially glycosylated in MCI hippocampus, with an observed increase associated with this neurodegenerative disorder. This finding validates our proteomics analysis and indicates that the WGA affinity column binds proteins with increased glycosylation levels. Thus, the WGA column is sensitive to changes to the extent of protein glycosylation.

DISCUSSION

Hippocampal and IPL brain sections taken from subjects with aMCI, AD, and age-matched, nondemented controls were homogenized, and proteins were fractionated with WGA affinity chromatography. Subsequent WGA affinity protein fractions from the aforementioned groups were compared using 2D proteomics techniques to assess changes in proteins with altered WGA affinity levels. To clarify the implications of altered WGA affinity protein levels, the overall level of 14-3-3γ and the level of N-acetylglucosamine linked 14-3-3γ were measured using Western blots. The results indicate that the WGA column binds proteins with altered extents of glycosylation with higher affinity independently of over-

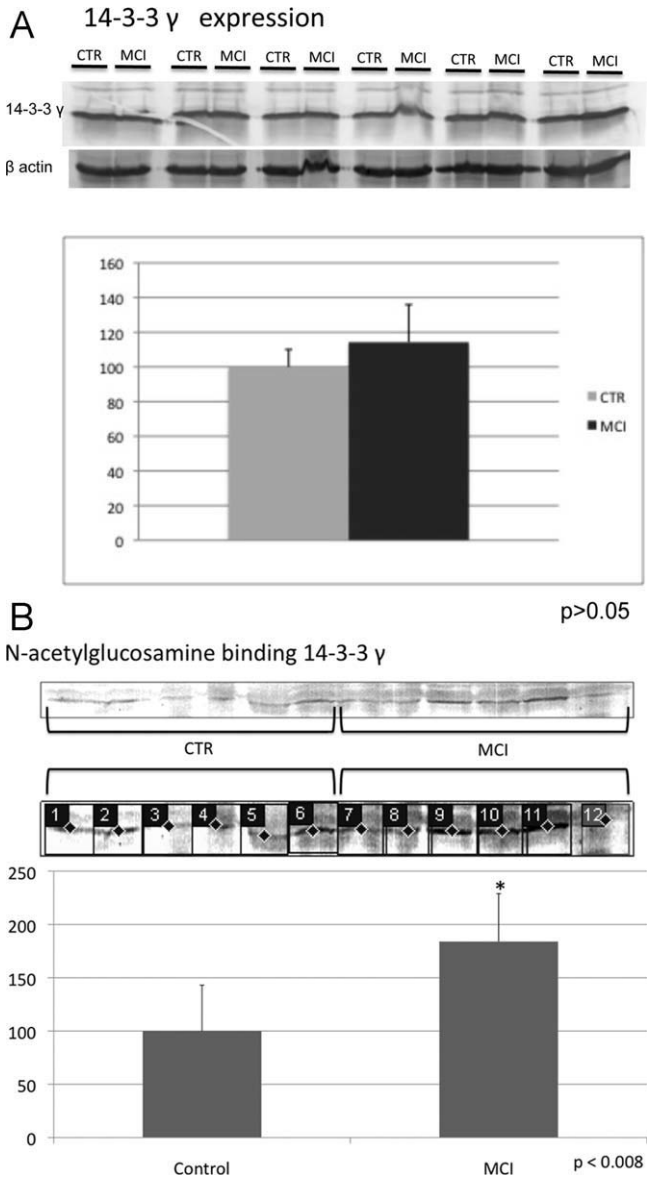

Fig. 4. **A:** Western blot image of 14-3-3γ levels and bar graph showing average control and MCI values. The graph shows no significant difference in the levels of 14-3-3γ, indicating that WGA column separation differences in MCI reflect differences in oligosaccharide levels. **B:** Western blot image of immunoprecipitated 14-3-3γ probed with anti-N-acetylglucosamine (O-GlcNAc) antibody and graph with average control and MCI values. The graph shows a significant difference in the extent of O-GlcNAc levels. An image is provided with lanes created in ImageQuant TL to provide clarity in band quantification.

all protein level. The results of the 14-3-3γ Western blot experiments also attest to WGA column affinity for N-acetylglucosamine carbohydrate moieties. Proteins found in the current study with altered WGA affinity encompass a broad range of functions, including chaperone, protein folding, glycoprotein maturation, metabolic, cytoskeletal and cytoskeletal maintenance, signaling, synaptic, secreted, and translational.

Chaperone and Glycoprotein Maturation Proteins

The ubiquitin/proteosome system (UPS), glucose metabolism, and Ca^{2+} homeostasis are disrupted in AD brain and are potent inducers of endoplasmic reticulum (ER) stress (Hoyer, 2004; Cecarini et al., 2007; Green, 2009). Accumulating evidence suggests that ER stress and subsequent activation of the unfolded protein response (UPR) occur in AD brain (Hoozemans et al., 2005, 2006, 2009). The UPR attenuates general protein synthesis followed by the up-regulation of chaperone proteins. The UPR will induce apoptosis if cellular homeostasis is not recovered (Vembar and Brodsky, 2008). The ER-resident chaperone proteins calreticulin, GP96, and protein disulfide isomerase (PDI) and the ER-resident protein glucosidase II were identified in the current study with alterations in WGA affinity. Calreticulin, GP96, and PDI are integral to proper protein folding of maturing glycoproteins and to proteins retrotranslocated to the ER (Krebs et al., 2004; Wu et al., 2006; Issad and Kuo, 2008; Vembar and Brodsky, 2008). GP96 is an HSP90 class chaperone protein but has an additional immunological role as an antigen-presenting molecule at the cell surface (Csermely et al., 1998). Also, the glycosylation level of GP96 has previously been reported to change as a function of cell stress and disease, including diabetes and cancer (Booth and Koch, 1989; Kang and Welch, 1991; Csermely et al., 1998). PDI catalyzes proper disulfide bond formation during protein maturation and repairs nonnative disulfide bonds that form as a consequence of cellular stresses to mature proteins. PTMs to PDI have been previously shown to alter cellular homeostasis dramatically. PDI-nitrosylation in AD brain has been shown to inhibit PDI activity (Uehara et al., 2006). In addition, PDI-nitrosylation leads to the accumulation of polyubiquitinated proteins and UPR activation (Uehara et al., 2006).

Glucosidase II facilitates the entrance and exit of proteins into and out of the calreticulin/calnexin cycle, which is a glycoprotein quality-control mechanism. Maturing glycoproteins undergo the dynamic addition and removal of terminal glucose residues to and from their glycan moiety, with the removal of glucose catalyzed by glucosidase I and II. When maturing glycoproteins contain a solitary terminal glucose residue in the glycan moiety of the subject glycoprotein, the protein enters the calreticulin/calnexin cycle, facilitating protein folding (Vembar and Brodsky, 2008). Once the glycoprotein reaches a properly folded conformation, glucosidase II trims the terminal glucose moiety of the glycan allowing the maturing glycoprotein to exit the calreticulin/calnexin cycle and proceed to the glycoprotein's appropriate destination.

Several ER-resident proteins found in the current study coupled with abundant literature relating these proteins to AD suggest that proteomics-identified ER proteins with altered WGA affinity play a role in ER stress observed in AD. Further studies are required to elucidate the implications of altered WGA affinity in AD, but we speculate that alterations in WGA affinity reflect these

proteins' inability properly to bind target proteins and inhibit chaperone and glycosylation activities.

Metabolic Proteins

The current proteomics study identified two metabolic proteins with altered WGA affinity, γ-enolase and glutamate dehydrogenase (GDH). γ-Enolase is a neuron-specific glycolytic enzyme, but γ-enolase has numerous functions in addition to glycolysis (Butterfield and Lange, 2009). For example, γ-enolase functions in neurons to regulate membrane-bound plasminogen, which is further cleaved to form plasmin (Butterfield and Lange, 2009), with the latter shown to degrade both oligomeric and fibrillary Aβ, thereby blocking Aβ-induced neurotoxicity (Van Nostrand and Porter, 1999). γ-Enolase has previously been shown to be glycosylated, supporting the findings of the current study (Wells et al., 2002; Vosseller et al., 2005).

GDH is integral to maintaining glutamate homeostasis and potentially plays a role in the glutamate induced excitotoxicity observed in AD. The observed decrease in the levels of γ-enolase WGA affinity in MCI and AD hippocampus with the concomitant increase in GDH WGA affinity levels in both the aforementioned brain regions in the current study suggests a compensatory mechanism to cope with glucose metabolism deficits observed in AD brain. The changes observed in γ-enolase and GDH WGA affinity correlate strongly with decreased glucose metabolism and excitotoxicity observed in AD and are consistent with elevated Aβ in AD and MCI brain (Yamaguchi et al., 1997).

Cytoskeletal and Cytoskeletal Maintenance Proteins

Oxidative PTMs to structural and cytoskeletal proteins and to proteins responsible for the maintenance and assembly dynamics of such proteins in axons and synapses have been hypothesized to play a role in the conversion of aMCI to AD (Butterfield and Sultana, 2007). NFTs are composed of hyperphosphorylated tau, a microtubule-associated protein involved in microtubule assembly and stabilization. NFTs critically impair tau protein's ability to bind and stabilize microtubules disrupting the axonal cytoskeleton (Butterfield et al., 2006). Cytoskeletal proteins found in this study with altered WGA affinity interact with tau or are associated with NFTs. Structural proteins identified in the present proteomics study with altered WGA affinity are 14-3-3γ, 14-3-3ε, and tropomyosin 1 in aMCI and tropomyosin 2, gelsolin, and 14-3-3ζ in AD.

14-3-3 Proteins modulate metabolic, apoptotic, cell cycle, and transcription factor proteins in myriad ways (Yaffe, 2002). Previous studies on the localization and action of 14-3-3 in AD brain found that 14-3-3ζ is associated with NFTs and accelerates the PKA-catalyzed phosphorylation of tau, suggesting that 14-3-3ζ regulates microtubule assembly dynamics in the brain (Fu et al., 2000; Takahashi, 2003). Aberrant expression of 14-3-3ζ, 14-3-3ε, and 14-3-3γ has been shown in the CNS throughout the progression of several neurodegenerative diseases, including AD (Fountoulakis et al., 1999; Peyrl et al., 2002). The increased WGA affinity observed in the 14-3-3-class proteins identified in the current study may lead to conformational changes within the protein, modifying binding affinity and functionality, thereby providing potential mechanisms for studying the causality of aberrant 14-3-3 protein function observed in AD (Comer and Hart, 2000; Li and Paudel, 2007).

Tropomyosin (TPM) stabilizes both muscle and nonmuscle cell actin filaments (Nyakern-Meazza et al., 2002). Neuronal cells express a limited spectrum of TPM isoforms implicated in the differentiation and maturation of neurons as well as polarization of developing neurons, dendritic and axonal growth, and growth cone size and formation (Stamm et al., 1993; Gunning et al., 2008). TPMs have been shown to be an integral components of NFTs in AD (Galloway et al., 1990). Cytosolic gelsolin also interacts with actin, playing a role in modulating the length and number of actin filaments in neurons. TPMs and gelsolin work in concert to regulate microfilament assembly (Nyakern-Meazza et al., 2002). TPMs are capable of annealing gelsolin-severed actin filaments and are efficient in converting gelsolin-actin complexes into long actin filaments (Nyakern-Meazza et al., 2002). TPM and gelsolin levels increase during stress conditions in vitro and during AD progression, suggesting that both TPM and gelsolin are involved in the disease progression (Ji et al., 2009; Owen et al., 2009). The current study showed an increase in WGA affinity for TPM1 and TPM2 and a decrease in WGA affinity for gelsolin. This finding suggests that the balance of gelsolin-mediated actin severance and TPM-mediated actin repair is altered in AD hippocampus. As noted above, alterations to cytoskeletal and cytoskeletal maintenance proteins observed in the current study with altered WGA affinity have also been well documented in the AD literature as being dysfunctional. The findings of the current study provide a rationale for new avenues of research to account for the differences observed in cytoskeletal and cytoskeletal maintenance proteins in AD brain.

Synaptic Proteins

β-Synuclein belongs to a family of highly homologous soluble proteins abundantly expressed in neurons at presynaptic terminals, particularly in the neocortex, hippocampus, striatum, thalamus, and cerebellum regions (George, 2002; Murphy et al., 2000). Several lines of evidence suggest that β-synuclein acts as a chaperone-like protein in membrane-associated processes at the presynaptic terminal, possibly involving neurotransmitter vesicle docking to the presynaptic terminal (Boyd-Kimball et al., 2005). β-Synuclein has decreased expression in AD brain and has been found to be linked to Aβ in AD neurofibrillary lesions (Rockenstein et al., 2001). β-Synuclein is glycosylated by a single O-GlcNAc

moiety in rat synaptosomes (Cole and Hart, 2001; Boyd-Kimball et al., 2005). The current study shows a modest decrease in WGA affinity of β-synuclein and may indicate that β-synuclein is less glycosylated in AD. However, the exact function of β-synuclein and the involvement of β-synuclein in AD remain to be elucidated.

Calcium Signaling Proteins

The calcium hypothesis of AD concerns disrupted intracellular Ca^{2+} homeostasis leading to neuronal dysfunction and ultimately apoptosis (Khachaturian, 1989). Calmodulin (CaM) is an effector of calcium signaling and has a central role in neurodegenerative processes such as plasticity, learning, and memory (Klee et al., 1980; Sola et al., 1999). CaM participates in synaptic function and neurotransmitter release, playing a role in Ca^{2+}-stimulated phosphorylation of synaptic proteins (Delorenzo et al., 1982). In addition, CaM regulates the assembly and disassembly of microtubules (Marcum et al., 1978). Altered WGA affinity of CaM in AD brain relative to age-matched controls might decrease CaM protein binding affinity, potentially disrupting regulatory mechanisms of Ca^{2+} signaling (Sacks et al., 1992; Quadroni et al., 1994). Hence, altered WGA affinity of CaM in AD could be associated with altered CaM regulation of proteins.

Secreted and Translational Proteins

α1-Antichymotrypsin (ACT) is a secreted serine protease inhibitor and an acute-phase reactant protein (Ritchie et al., 2004; Licastro et al., 2005). Several studies showed that ACT is found specifically in both amorphous and classic plaques in AD brain (Abraham and Potter, 1989a,b). The presence of inflammatory proteins, including ACT, apolipoprotein E (ApoE), and complement in plaques led to the hypothesis that these proteins might serve to promote Aβ polymerization and amyloid formation (Abraham et al., 1988; McGeer et al., 1989; M.V. Aksenov et al., 1996; M.Y. Aksenov et al., 1996). The impact of altered WGA affinity on ACT function in AD is not clear; however, changes in glycan composition might affect ACT's structure and localization and contribute to functional alterations of inflammatory proteins in AD.

*N*2,*N*2-dimethylguanosine tRNA methyltransferase (DMGtRNAMT) is an intracellular enzyme involved in the maturation of tRNA. Previous studies show alterations at the ribosome level in MCI and AD subjects, including decreased rate and capacity for protein synthesis, decreased ribosomal RNA and tRNA levels, and increased RNA oxidation (Ding et al., 2006). Further studies are needed to understand the involvement of altered WGA affinity DMGtRNAMT in AD, but we speculate that such PTM differences in AD may be related to the altered protein synthesis reported to exist (Ding et al., 2006).

SUMMARY

The altered WGA affinities of the proteins identified in the current proteomics study correlate strongly with previously established criteria and studies of glycosylation of these proteins. Also, as discussed above, most of the proteins found in the current study have been previously reported to be involved in pathways associated with cellular insults present in AD brain. Further characterization is needed to understand fully the implications of altered WGA affinity of these proteins, but a potential mechanism for further study is O-GlcNAcylation. The proteins found in the current study are all known to be phosphorylated and are localized in cytoplasmic, ER lumen, and the endomembrane system. To date, all known O-GlcNAc proteins are also phosphoproteins, suggesting that proteins identified in the current study are potentially modified by O-GlcNAc (Hart et al., 1996). It is important to note that possibilities exist that proteins found in this study are modified by sialic acid or have an increased affinity for the WGA lectin binding domain; however, the findings in the current proteomics study correlate well with the established criteria for O-GlcNAcylation and the AD literature.

REFERENCES

Abraham CR, Potter H. 1989a. Alpha 1-antichymotrypsin in brain aging and disease. Prog Clin Biol Res 317:1037–1048.

Abraham CR, Potter H. 1989b. The protease inhibitor, alpha 1-antichymotrypsin, is a component of the brain amyloid deposits in normal aging and Alzheimer's disease. Ann Med 21:77–81.

Abraham CR, Selkoe DJ, Potter H. 1988. Immunochemical identification of the serine protease inhibitor alpha 1-antichymotrypsin in the brain amyloid deposits of Alzheimer's disease. Cell 52:487–501.

Aksenova MV, Aksenov MY, Butterfield DA, Carney JM. 1996. Alpha-1-antichymotrypsin interaction with A beta (1–40) inhibits fibril formation but does not affect the peptide toxicity. Neurosci Lett 211:45–48.

Aksenov MY, Aksenova MV, Carney JM, Butterfield DA. 1996. Alpha 1-antichymotrypsin interaction with A beta (1–42) does not inhibit fibril formation but attenuates the peptide toxicity. Neurosci Lett 217:117–120.

Boguski MS, McIntosh MW. 2003. Biomedical informatics for proteomics. Nature 422:233–237.

Booth C, Koch GL. 1989. Perturbation of cellular calcium induces secretion of luminal ER proteins. Cell 59:729–737.

Boyd-Kimball D, Sultana R, Poon HF, Lynn BC, Casamenti F, Pepeu G, Klein JB, Butterfield DA. 2005. Proteomic identification of proteins specifically oxidized by intracerebral injection of amyloid beta-peptide (1–42) into rat brain: implications for Alzheimer's disease. Neuroscience 132:313–324.

Butterfield DA, Lange ML. 2009. Multifunctional roles of enolase in Alzheimer's disease brain: beyond altered glucose metabolism. J Neurochem 111:915–933.

Butterfield DA, Sultana R. 2007. Redox proteomics identification of oxidatively modified brain proteins in Alzheimer's disease and mild cognitive impairment: insights into the progression of this dementing disorder. J Alzheimers Dis 12:61–72.

Butterfield DA, Abdul HM, Opii W, Newman SF, Joshi G, Ansari MA, Sultana R. 2006. Pin1 in Alzheimer's disease. J Neurochem 98:1697–1706.

Cecarini V, Ding Q, Keller JN. 2007. Oxidative inactivation of the proteasome in Alzheimer's disease. Free Radic Res 41:673–680.

Clower DM, West RA, Lynch JC, Strick PL. 2001. The inferior parietal lobule is the target of output from the superior colliculus, hippocampus, and cerebellum. J Neurosci 21:6283–6291.

Cole RN, Hart GW. 2001. Cytosolic O-glycosylation is abundant in nerve terminals. J Neurochem 79:1080–1089.

Comer FI, Hart GW. 2000. O-Glycosylation of nuclear and cytosolic proteins. Dynamic interplay between O-GlcNAc and O-phosphate. J Biol Chem 275:29179–29182.

Csermely P, Schnaider T, Soti C, Prohaszka Z, Nardai G. 1998. The 90-kDa molecular chaperone family: structure, function, and clinical applications. A comprehensive review. Pharmacol Ther 79:129–168.

Delorenzo RJ, Gonzalez B, Goldenring J, Bowling A, Jacobson R. 1982. Ca^{2+}-calmodulin tubulin kinase system and its role in mediating the Ca^{2+} signal in brain. Prog Brain Res 56:257–286.

Ding Q, Markesbery WR, Cecarini V, Keller JN. 2006. Decreased RNA, and increased RNA oxidation, in ribosomes from early Alzheimer's disease. Neurochem Res 31:705–710.

Fountoulakis M, Cairns N, Lubec G. 1999. Increased levels of 14-3-3 gamma and epsilon proteins in brain of patients with Alzheimer's disease and Down syndrome. J Neural Transm Suppl 57:323–335.

Fu H, Subramanian RR, Masters SC. 2000. 14-3-3 Proteins: structure, function, and regulation. Annu Rev Pharmacol Toxicol 40:617–647.

Galloway PG, Mulvihill P, Siedlak S, Mijares M, Kawai M, Padget H, Kim R, Perry G. 1990. Immunochemical demonstration of tropomyosin in the neurofibrillary pathology of Alzheimer's disease. Am J Pathol 137:291–300.

George JM. 2002. The synucleins. Genome Biol 3:3002.

Green KN. 2009. Calcium in the initiation, progression and as an effector of Alzheimer's disease pathology. J Cell Mol Med 13:2787–2799.

Gunning P, O'Neill G, Hardeman E. 2008. Tropomyosin-based regulation of the actin cytoskeleton in time and space. Physiol Rev 88:1–35.

Hart GW. 1997. Dynamic O-linked glycosylation of nuclear and cytoskeletal proteins. Annu Rev Biochem 66:315–335.

Hart GW, Kreppel LK, Comer FI, Arnold CS, Snow DM, Ye Z, Cheng X, DellaManna D, Caine DS, Earles BJ, Akimoto Y, Cole RN, Hayes BK. 1996. O-GlcNAcylation of key nuclear and cytoskeletal proteins: reciprocity with O-phosphorylation and putative roles in protein multimerization. Glycobiology 6:711–716.

Hart GW, Housley MP, Slawson C. 2007. Cycling of O-linked beta-N-acetylglucosamine on nucleocytoplasmic proteins. Nature 446:1017–1022.

Hoozemans JJ, Veerhuis R, Van Haastert ES, Rozemuller JM, Baas F, Eikelenboom P, Scheper W. 2005. The unfolded protein response is activated in Alzheimer's disease. Acta Neuropathol 110:165–172.

Hoozemans JJ, Stieler J, van Haastert ES, Veerhuis R, Rozemuller AJ, Baas F, Eikelenboom P, Arendt T, Scheper W. 2006. The unfolded protein response affects neuronal cell cycle protein expression: implications for Alzheimer's disease pathogenesis. Exp Gerontol 41:380–386.

Hoozemans JJ, van Haastert ES, Nijholt DA, Rozemuller AJ, Eikelenboom P, Scheper W. 2009. The unfolded protein response is activated in pretangle neurons in Alzheimer's disease hippocampus. Am J Pathol 174:1241–1251.

Hoyer S. 2004. Causes and consequences of disturbances of cerebral glucose metabolism in sporadic Alzheimer disease: therapeutic implications. Adv Exp Med Biol 541:135–152.

Issad T, Kuo M. 2008. O-GlcNAc modification of transcription factors, glucose sensing and glucotoxicity. Trends Endocrinol Metab 19:380–389.

Ji L, Chauhan A, Muthaiyah B, Wegiel J, Chauhan V. 2009. Gelsolin levels are increased in the brain as a function of age during normal development in children that are further increased in Down syndrome. Alzheimer Dis Assoc Disord 23:319–322.

Kang HS, Welch WJ. 1991. Characterization and purification of the 94-kDa glucose-regulated protein. J Biol Chem 266:5643–5649.

Khachaturian ZS. 1989. Calcium, membranes, aging, and Alzheimer's disease. Introduction and overview. Ann N Y Acad Sci 568:1–4.

Klee CB, Crouch TH, Richman PG. 1980. Calmodulin. Annu Rev Biochem 49:489–515.

Krebs MP, Noorwez SM, Malhotra R, Kaushal S. 2004. Quality control of integral membrane proteins. Trends Biochem Sci 29:648–655.

Lefebvre T, Dehennaut V, Guinez C, Olivier S, Drougat L, Mir AM, Mortuaire M, Vercoutter-Edouart AS, Michalski JC. 2010. Dysregulation of the nutrient/stress sensor O-GlcNAcylation is involved in the etiology of cardiovascular disorders, type-2 diabetes and Alzheimer's disease. Biochim Biophys Acta 1800:67–79.

Li T, Paudel HK. 2007. 14-3-3Zeta facilitates GSK3beta-catalyzed tau phosphorylation in HEK-293 cells by a mechanism that requires phosphorylation of GSK3beta on Ser9. Neurosci Lett 414:203–208.

Licastro F, Chiappelli M, Grimaldi LM, Morgan K, Kalsheker N, Calabrese E, Ritchie A, Porcellini E, Salani G, Franceschi M, Canal N. 2005. A new promoter polymorphism in the alpha-1-antichymotrypsin gene is a disease modifier of Alzheimer's disease. Neurobiol Aging 26:449–453.

Liu F, Iqbal K, Grundke-Iqbal I, Hart GW, Gong CX. 2004. O-GlcNAcylation regulates phosphorylation of tau: a mechanism involved in Alzheimer's disease. Proc Natl Acad Sci U S A 101:10804–10809.

Marcum JM, Dedman JR, Brinkley BR, Means AR. 1978. Control of microtubule assembly-disassembly by calcium-dependent regulator protein. Proc Natl Acad Sci U S A 75:3771–3775.

Markesbery WR. 1997. Neuropathological criteria for the diagnosis of Alzheimer's disease. Neurobiol Aging 18(Suppl):S13–S19.

Maurer HH, Peters FT. 2005. Toward high-throughput drug screening using mass spectrometry. Ther Drug Monit 27:686–688.

McGeer PL, Akiyama H, Itagaki S, McGeer EG. 1989. Activation of the classical complement pathway in brain tissue of Alzheimer patients. Neurosci Lett 107:341–346.

Mebane-Sims I. 2009. Alzheimer's disease facts and figures. Alzheimers Dement 5:234–270.

Murphy DD, Rueter SM, Trojanowski JQ, Lee VM. 2000. Synucleins are developmentally expressed, and alpha-synuclein regulates the size of the presynaptic vesicular pool in primary hippocampal neurons. J Neurosci 20:3214–3220.

Nyakern-Meazza M, Narayan K, Schutt CE, Lindberg U. 2002. Tropomyosin and gelsolin cooperate in controlling the microfilament system. J Biol Chem 277:28774–28779.

Owen JB, Di Domenico F, Sultana R, Perluigi M, Cini C, Pierce WM, Butterfield DA. 2009. Proteomics-determined differences in the concanavalin-A-fractionated proteome of hippocampus and inferior parietal lobule in subjects with Alzheimer's disease and mild cognitive impairment: implications for progression of AD. J Proteome Res 8:471–482.

Peyrl A, Weitzdoerfer R, Gulesserian T, Fountoulakis M, Lubec G. 2002. Aberrant expression of signaling-related proteins 14-3-3 gamma and RACK1 in fetal Down syndrome brain (trisomy 21). Electrophoresis 23:152–157.

Quadroni M, James P, Carafoli E. 1994. Isolation of phosphorylated calmodulin from rat liver and identification of the in vivo phosphorylation sites. J Biol Chem 269:16116–16122.

Ritchie A, Morgan K, Kalsheker N. 2004. Allele-specific overexpression in astrocytes of an Alzheimer's disease associated alpha-1-antichymotrypsin promoter polymorphism. Brain Res Mol Brain Res 131:88–92.

Rockenstein E, Hansen LA, Mallory M, Trojanowski JQ, Galasko D, Masliah E. 2001. Altered expression of the synuclein family mRNA in Lewy body and Alzheimer's disease. Brain Res 914:48–56.

Sacks DB, Davis HW, Williams JP, Sheehan EL, Garcia JG, McDonald JM. 1992. Phosphorylation by casein kinase II alters the biological activity of calmodulin. Biochem J 283:21–24.

Selkoe DJ. 2004. Cell biology of protein misfolding: the examples of Alzheimer's and Parkinson's diseases. Nat Cell Biol 6:1054–1061.

Sola C, Barron S, Tusell JM, Serratosa J. 1999. The Ca^{2+}/calmodulin signaling system in the neural response to excitability. Involvement of neuronal and glial cells. Prog Neurobiol 58:207–232.

Stamm S, Casper D, Lees-Miller JP, Helfman DM. 1993. Brain-specific tropomyosins TMBr-1 and TMBr-3 have distinct patterns of expression during development and in adult brain. Proc Natl Acad Sci U S A 90: 9857–9861.

Takahashi Y. 2003. The 14-3-3 proteins: gene, gene expression, and function. Neurochem Res 28:1265–1273.

Thongboonkerd V, McLeish KR, Arthur JM, Klein JB. 2002. Proteomic analysis of normal human urinary proteins isolated by acetone precipitation or ultracentrifugation. Kidney Int 62:1461–1469.

Uehara T, Nakamura T, Yao D, Shi ZQ, Gu Z, Ma Y, Masliah E, Nomura Y, Lipton SA. 2006. S-nitrosylated protein-disulphide isomerase links protein misfolding to neurodegeneration. Nature 441:513–517.

Van Nostrand WE, Porter M. 1999. Plasmin cleavage of the amyloid beta-protein: alteration of secondary structure and stimulation of tissue plasminogen activator activity. Biochemistry 38:11570–11576.

Vembar SS, Brodsky JL. 2008. One step at a time: endoplasmic reticulum-associated degradation. Nat Rev Mol Cell Biol 9:944–957.

Vosseller K, Hansen KC, Chalkley RJ, Trinidad JC, Wells L, Hart GW, Burlingame AL. 2005. Quantitative analysis of both protein expression and serine/threonine post-translational modifications through stable isotope labeling with dithiothreitol. Proteomics 5:388–398.

Wells L, Vosseller K, Cole RN, Cronshaw JM, Matunis MJ, Hart GW. 2002. Mapping sites of O-GlcNAc modification using affinity tags for serine and threonine post-translational modifications. Mol Cell Proteomics 1:791–804.

Wu JC, Liang ZQ, Qin ZH. 2006. Quality control system of the endoplasmic reticulum and related diseases. Acta Biochim Biophys Sin 38: 219–226.

Yaffe MB. 2002. How do 14-3-3 proteins work? Gatekeeper phosphorylation and the molecular anvil hypothesis. FEBS Lett 513:53–57.

Yamaguchi S, Meguro K, Itoh M, Hayasaka C, Shimada M, Yamazaki H, Yamadori A. 1997. Decreased cortical glucose metabolism correlates with hippocampal atrophy in Alzheimer's disease as shown by MRI and PET. J Neurol Neurosurg Psychiatry 62:596–600.